

Do *S,S'*-Coordinated *o*-Dithiobenzosemiquinonate(1⁻) Radicals Exist in Coordination Compounds? The [Au^{III}(1,2-C₆H₄S₂)₂]^{1-/0} CoupleKallol Ray,[†] Thomas Weyhermüller,[†] Anton Goossens,^{‡,§} Menno W. J. Crajé,[§] and Karl Wieghardt^{*†}

Max-Planck-Institut für Strahlenchemie, Stiftstrasse 34-36, D-45470 Mülheim an der Ruhr, Germany, Kamerlingh Onnes Laboratorium, University of Leiden, P.O. Box 9504, 2300 RA Leiden, The Netherlands, and Interfacultair Reactor Instituut, Delft University of Technology, Mekelweg 15, 2629 JB Delft, The Netherlands

Received December 9, 2002

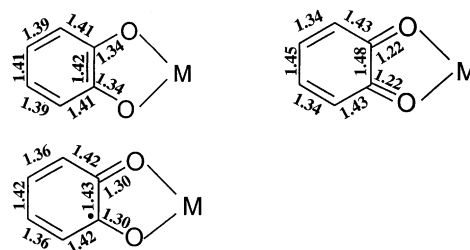
The square planar, light-green, diamagnetic complex [N(*n*-Bu)₄][Au^{III}(L^{*t*}-Bu)₂] (**1**) reacts with iodine in acetone affording the neutral paramagnetic species [Au(L^{*t*}-Bu)₂] (**1a**) (*S* = 1/2) where H₂[L^{*t*}-Bu] represents the ligand 3,5-di-*tert*-butyl-1,2-benzenedithiol. The corresponding complexes containing the unsubstituted ligand H₂[L], 1,2-benzenedithiol, namely [N(*n*-Bu)₄][Au(L)₂] (**2**) and [Au(L)₂] (**2a**), have also been prepared and characterized by X-ray crystallography; the structure of the latter has been reported in ref 10. ¹⁹⁷Au Mössbauer spectra of **1** and **1a** clearly show that the one-electron oxidation is ligand-centered and does not involve the formation of Au(IV) (*d*⁷). The spectroscopic features of the ligand mixed-valent species **1a** were determined by UV–vis, EPR, and IR spectroscopy which allows the detection of *S,S*-coordinated 1,2-dithiobenzosemiquinonate(1⁻) radicals in coordination compounds.

Introduction

The coordination chemistry of O,O'-coordinated *o*-benzosemiquinonate(1⁻) π radicals is well established and understood.¹ A variety of typical structural and spectroscopic features have been identified which allow the unequivocal detection and characterization of such species in a given coordination compound.² Probably the most reliable single feature in this respect is the metrical parameters of such a species as shown schematically in Scheme 1 for the three differing oxidation levels of O,O-coordinated (i) catecholate(2⁻), (ii) benzosemiquinonate(1⁻), and (iii) benzoquinone.

The situation is not so clear for the corresponding *o*-dithio derivatives. Thus, the existence of *S,S*-coordinated *o*-dithiobenzosemiquinonate(1⁻) radical anions (rather than their closed-shell, aromatic *o*-dithiolate(2⁻) dianions) has been suggested to occur in some complexes,³ but it has more recently been explicitly ruled out.⁴ Clear experimental

Scheme 1



evidence for its presence has been presented for paramagnetic square planar [Pd(bpy)(L^{*t*}-Bu)]⁺ (*S* = 1/2) for which an electronic spectrum and an EPR spectrum have been recorded which are compatible only with the presence of an *o*-dithiobenzosemiquinonate(1⁻) radical.⁵ (L^{*t*}-Bu)²⁻ represents Sellmann's 3,5-di-*tert*-butylbenzodithiolate(2⁻) ligand⁶ and (L)²⁻ is the unsubstituted 1,2-benzenedithiolate(2⁻) dianion.

Recent DFT calculations have convincingly shown⁷ that the spectroscopic oxidation state of the central nickel ion in

* To whom correspondence should be addressed. E-mail: wieghardt@mpi-muelheim.mpg.de.

[†] MPI Mülheim.

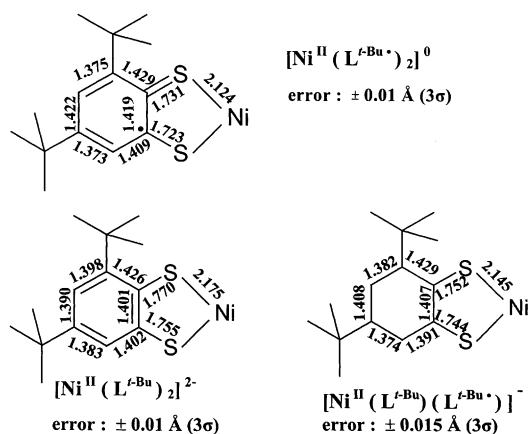
[‡] University of Leiden.

[§] Delft University of Technology.

- (1) (a) Pierpont, C. G.; Buchanan, R. M. *Coord. Chem. Rev.* **1981**, *38*, 45. (b) Pierpont, C. G.; Lange, C. W. *Prog. Inorg. Chem.* **1994**, *41*, 331. (c) Pierpont, C. G.; Attia, A. S. *Collect. Czech. Chem. Commun.* **2001**, *66*, 33.
- (2) Bhattacharya, S.; Gupta, P.; Basuli, F.; Pierpont, C. G. *Inorg. Chem.* **2002**, *41*, 5810.
- (3) Sawyer, D. T.; Srivatsa, G. S.; Bodini, M. E.; Schaefer, W. P.; Wing, R. M. *J. Am. Chem. Soc.* **1986**, *108*, 936.

- (4) (a) Sellmann, D.; Geck, M.; Knoch, F.; Ritter, G.; Dengler, J. *J. Am. Chem. Soc.* **1991**, *113*, 3819. (b) Sellmann, D.; Binder, H.; Häussinger, D.; Heinemann, F. W.; Sutter, J. *Inorg. Chim. Acta* **2000**, *300–302*, 829.
- (5) Ghosh, P.; Begum, A.; Herebian, D.; Bothe, E.; Hildenbrand, K.; Weyhermüller, T.; Wieghardt, K. *Angew. Chem.* **2003**, *115*, 581; *Angew. Chem., Int. Ed.* **2003**, *42*, 563.
- (6) (a) Sellmann, D.; Freyberger, G.; Eberlein, R.; Böhlen, E.; Huttner, G.; Zsolnai, L. *J. Organomet. Chem.* **1987**, *323*, 21. (b) Sellmann, D.; Käßler, O. *Z. Naturforsch.* **1987**, *42b*, 1291.
- (7) Bachler, V.; Olbrich, G.; Neese, F.; Wieghardt, K. *Inorg. Chem.* **2002**, *41*, 4179.

Scheme 2



diamagnetic, square planar $[\text{Ni}(\text{L}^*)_2]$ is $+\text{II}$ (d^8), and the two equivalent ligands are therefore *o*-dithiobenzosemiquinonates($1-$).⁷ The complex $[\text{Ni}^{\text{II}}(\text{L}^{\text{t-Bu}^*})_2]$ has been characterized by X-ray crystallography as having its mono- and dianionic counterparts.^{4b} The latter complex $[\text{Ni}^{\text{II}}(\text{L}^{\text{t-Bu}^*})_2]^{2-}$ contains undoubtedly two dithiolato($2-$) ligands. The established structural features shown in Scheme 2 for *o*-dithiobenzosemiquinonates($1-$) and *o*-dithiocatecholates($2-$) allow, in principle, again unambiguous assignment of the oxidation level of an *o*-dithiolate ligand in a given complex provided that a high-quality crystal structure with experimental errors for the C–C and C–S bond lengths of maximally $\pm 0.01 \text{ \AA}$ ($\equiv 3\sigma$) is available. Many crystal structures of bis(dithiolato)-metal complexes have appeared in the literature which do not meet this quality criterion.⁸ Therefore, the correct electronic structures of many of these complexes remain to be established.

This problem is even amplified in complexes where *o*-dithiobenzosemiquinonate ligands and, in addition, *o*-dithiolates are bound to the same metal ion. The structural differences between the two ligand types are small,^{4b} and therefore, static disorder problems may hamper their identification by crystallography.

On the other hand, it is also often possible to establish the d^n electron configuration of the central transition metal ion by spectroscopic methods (electronic, EPR, and Mössbauer spectroscopy, etc.) which in turn defines the oxidation level of the ligands.

Here, we establish the electronic structure of the bis(*o*-dithiolato)gold(III) anion and its one-electron oxidized neutral form which has been described as a Au(IV) species implying thereby a d^7 electron configuration of the central gold ion. A number of low-quality crystal structures of salts containing the $[\text{Au}^{\text{III}}(\text{L}_2)]^-$ monoanion have been reported,⁹ but these

do not allow an unambiguous assignment of the ligand as *o*-dithiolato($2-$) dianion.⁹ Interestingly, the crystal structure of $[\text{Au}^{\text{III}}(\text{L}_2)]$ has also been published (as Au(IV)!).^{10a} This structure is of medium quality and appears to imply the presence of one *o*-dithiobenzosemiquinonate($1-$) radical. In a subsequent paper, it has been shown^{10b} that the neutral complex $[\text{Au}(\text{L}_2)]$ is diamagnetic in the solid state and that the square planar units form nearly uniform stacks of $[\text{Au}(\text{L}_2)]$ molecules with a weak superstructure due to dimer formation. Ab initio calculations on isolated $[\text{Au}^{\text{III}}(\text{L}_2)]$ molecules have suggested that “the highest occupied and singly occupied molecular orbitals (HOMO and SOMO) are almost the pure bonding and antibonding combinations of the ligand HOMOs.”¹⁴ This requires a diamagnetic Au(III) ion with a d^8 electron configuration. No experimental data have been reported to date which prove this point.

We will show here that the electronic structure of the paramagnetic, new neutral species $[\text{Au}(\text{L}^{\text{t-Bu}^*})_2]$ can only be understood in terms of a Au(III) (d^8 , $S = 0$) ion S,S-coordinated to one *o*-dithiolato dianion ($\text{L}^{\text{t-Bu}^*})^{2-}$ and an *o*-dithiobenzosemiquinonate($1-$) π radical, ($\text{L}^{\text{t-Bu}^*})^{1-}$ yielding an $S = 1/2$ ground state. The two *tert*-butyl groups per S,S-coordinated ligand effectively prevent stacking interactions between $[\text{Au}(\text{L}^{\text{t-Bu}^*})_2]$ molecules in the solid state.

Experimental Section

The ligand 3,5-di-*tert*-butyl-1,2-benzenedithiol, $\text{H}_2[\text{L}^{\text{t-Bu}^*}]$, has been prepared as described in the literature.⁶ 1,2-Benzenedithiol, $\text{H}_2[\text{L}]$, is commercially available.

$[\text{N}(n\text{-Bu})_4][\text{Au}^{\text{III}}(\text{L}^{\text{t-Bu}^*})_2]$ (**1**). Sodium metal (0.069 g; 3.0 mmol) was added to a solution of $[\text{N}(n\text{-Bu})_4]\text{Br}$ (0.161 g; 0.5 mmol) and $\text{H}_2[\text{L}^{\text{t-Bu}^*}]$ (0.25 g; 1.0 mmol) in absolute ethanol (10 mL). A solution of $\text{Na}[\text{AuCl}_4] \cdot 2\text{H}_2\text{O}$ (0.20 g; 0.5 mmol) in ethanol (8 mL) was slowly added to the above solution at ambient temperature. A green precipitate formed within 30 min which was collected by filtration, washed with diethyl ether, and air-dried. The crude product was recrystallized from CH_2Cl_2 solution yielding shining light-green microcrystals of **1** (0.34 g, 72%). Anal. Calcd for $\text{C}_{44}\text{H}_{76}\text{S}_4\text{NAu}$: C, 55.97; H, 8.11; N, 1.48. Found: C, 55.9; H, 8.3; N, 1.5. Electrospray mass spectrum (CH_2Cl_2 solution): $m/z = 700.7 \{M\}^-$, $242.3 \{M\}^+$.

$[\text{Au}(\text{L}^{\text{t-Bu}^*})_2]$ (**1a**). To a light green solution of **1** (60 mg; 0.063 mmol) in dry acetone (5 mL) under an argon blanketing atmosphere was added dropwise a solution of iodine (31 mg; 0.12 mmol) in acetone (5 mL) with stirring at 20 °C. A yellowish-green microcrystalline solid precipitated immediately. During addition, the solution must be rigorously stirred. We have not found a suitable solvent in which **1a** is stable and, therefore, have not been able to recrystallize the material. Yield: 21 mg (50%). Anal. Calcd for

(8) (a) Eisenberg, R. *Prog. Inorg. Chem.* **1970**, *12*, 295. (b) Holm, R. H.; O'Connor, M. J. *Prog. Inorg. Chem.* **1971**, *14*, 241.

(9) Crystal structures of salts containing the $[\text{Au}^{\text{III}}(\text{L}_2)]^-$ anion: (a) Mazid, M. A.; Razi, M. T.; Sadler, P. J. *Inorg. Chem.* **1981**, *20*, 2872. (b) Nakamoto, M.; Koijman, H.; Paul, M.; Hiller, W.; Schmidbaur, H. *Z. Anorg. Allg. Chem.* **1993**, *619*, 1341. (c) Davila, R. M.; Staples, R. J.; Fackler, J. P., Jr. *Acta Crystallogr., Sect. C* **1994**, *C50*, 1898. (d) Gimeno, M. C.; Jones, P. G.; Laguna, A.; Laguna, M.; Terroba, R. *Inorg. Chem.* **1994**, *33*, 3932. (e) Staples, R. J.; Fackler, J. P., Jr.; Davila, R. M.; Albreit, T. E. *Z. Kristallogr.* **1995**, *210*, 383.

(10) (a) Rindorf, G.; Thorup, N.; Bjørnholm, T.; Bechgaard, K. *Acta Crystallogr., Sect. C* **1990**, *C46*, 1437. (b) Schiødt, N. C.; Bjørnholm, T.; Bechgaard, K.; Neumeier, J. J.; Allgeier, C.; Jacobsen, C. S.; Thorup, N. *Phys. Rev. B* **1996**, *53*, 1773.

(11) Spek, A. L. *Platon 99 for Windows*; Utrecht University: Utrecht, The Netherlands, 1999.

(12) *ShelXTL V.5*; Siemens Analytical X-ray Instruments, Inc.: Madison, WI, 1994.

(13) Goossens, A.; Crajé, M. W. J.; van der Kraan, A. M.; Zwijnenburg, A.; Mackkee, M.; Monlijn, J. A.; de Jongh, L. J. *Catal. Today* **2002**, *72*, 95.

(14) Schiødt, N. C.; Sommer-Larsen, P.; Bjørnholm, T.; Nielsen, M. F.; Larsen, J.; Bechgaard, K. *Inorg. Chem.* **1995**, *34*, 3688.

Table 1. Crystal Data and Structure Refinement for **2**

formula	C ₂₄ H ₃₆ NS ₄ Au
fw	663.74
T	100(2) K
wavelength, Å	0.71073
cryst syst	triclinic
space group	P1
unit cell dimensions	$a = 7.5989(3)$ Å $b = 13.0465(6)$ Å $c = 14.7616(6)$ Å $\alpha = 68.04(1)^\circ$ $\beta = 76.53(1)^\circ$ $\gamma = 85.24(1)^\circ$
V, Z	1319.9(1) Å ³ , 2
D (calcd)	1.670 Mg m ⁻³
abs coeff	5.901 mm ⁻¹
F(000)	660
cryst size	0.53 × 0.42 × 0.23 mm ³
θ range for data collection	3.05–31.03°
index ranges	$-11 \leq h \leq 11$ $-18 \leq k \leq 18$ $-21 \leq l \leq 21$
reflns collected	42351
indep reflns	8385 ($R_{\text{int}} = 0.0445$)
max and min transm	0.344 and 0.146
refinement method	full-matrix least-squares on F^2
data/restraints/params	8385/0/281
GOF on F^2	1.097
final R indices	R1 = 0.0214, wR2 = 0.0562
[$I > 2\sigma(I)$]	
R indices (all data)	R1 = 0.0239, wR2 = 0.0575
largest diff peak and hole	2.459 and -2.525 e Å ⁻³

C₂₈H₄₀S₄Au: C, 47.92; H, 5.74. Found: C, 47.8; H, 5.75. EI mass spectrum: $m/z = 701$ {M}⁺.

[N(*n*-Bu)₃H][Au(L)₂] (2). To a solution of the ligand H₂[L] (0.14 g; 1.0 mmol) in absolute ethanol (5 mL) was added N(*n*-C₄H₉)₃ (0.37 g; 3 mmol). A solution of Na[AuCl₄]·2H₂O (0.20 g; 0.5 mmol) in ethanol (5 mL) was added dropwise at 20 °C with stirring under an Ar blanketing atmosphere to the described solution. A green solid precipitated immediately and was collected by filtration. Single crystals of **2** suitable for X-ray crystallography were obtained by recrystallization of the crude product from a 1:1 mixture (volume) of CH₂Cl₂ and toluene within 2 days. Anal. Calcd for C₂₄H₃₆NS₄Au: C, 43.43; H, 5.47; N, 2.11. Found: C, 43.3; H, 5.5; N, 2.0.

[Au(L)₂] (2a). This complex has been prepared electrochemically in ref 10. Its crystal structure has also been reported.

X-ray Crystallography Data Collection and Refinement of the Structure of 2. A transparent green crystal of **2** was coated with perfluoropolyether, picked up with a glass fiber, and mounted in the nitrogen cold stream of a Nonius-CCD diffractometer. Intensity data were collected at 100 K using graphite monochromated Mo K α ($\lambda = 0.71073$ Å) of a rotating anode source working at 50 kV/50 mA. Data collection was performed by taking 1299 frames at 5 s exposure and 1.00° rotation in ω . Final cell constants were obtained from a least-squares fit of 42351 reflections. The semiempirical absorption correction routine MulScanAbs¹¹ was used to account for absorption. The ShelXTL¹² software package was used for solution, refinement, and artwork of the structure which was readily solved by Patterson methods and difference Fourier techniques. All non-hydrogen atoms were refined anisotropically. Hydrogen atoms bound to carbon were placed at calculated positions and refined as riding atoms with isotropic displacement parameters. Hydrogen atom H(20) bound to N(20) was located from the difference map and isotropically refined. Crystallographic data of the compound are listed in Table 1.

Physical Measurements. Mössbauer spectra have been recorded in transmission geometry. The applied ¹⁹⁷Au gamma ray sources were obtained by irradiating enriched platinum powder (97.4% ¹⁹⁶Pt) with thermal neutrons for 24 h. This results in a 200 MBq Mössbauer source due to the reaction ¹⁹⁶Pt + n → ¹⁹⁷Pt, followed by ¹⁹⁷Pt → ¹⁹⁷Au + β^- + $\bar{\nu}_e$ + 0.6 MeV. The β decay process has a half-life of 18.3 h and determines the half-life of the ¹⁹⁷Au Mössbauer source. The ¹⁹⁷Au nucleus, left behind in an excited state, decays to the ground state by emission of the 77.3 keV γ photon that is used for Mössbauer spectroscopy. Both source and absorber were cooled to a temperature of 4.2 K. The source velocity has been calibrated by a Michelson interferometer.¹³ All isomer shift values are given according to this (absolute) scale. For detection of the transmitted photons, a high purity Ge detector has been used. Electronic spectra of complexes in solution were recorded on a scanning double beam UV–vis–NIR spectrophotometer (Perkin-Elmer, Lambda 19) in the range 200–2000 nm. Cyclic voltammograms and coulometric measurements were performed by using an EG&G potentiostat/galvanostat (model-273A). Temperature-dependent (2–298 K) magnetization data were measured on a SQUID magnetometer (MPMS Quantum design) in an external magnetic field of 1.0 T. The experimental susceptibility data were corrected for underlying diamagnetism by use of tabulated Pascal's constants. X-band EPR spectra were recorded on a Bruker ESP 300 spectrometer. The Fourier transform infrared spectra (KBr disks) were recorded on a Perkin-Elmer 2000 FT-IR instrument.

Results and Discussion

The reaction of disodium (3,5-di-*tert*-butyl-1,2-benzenedithiolate), Na₂[L^{*t*-Bu}], with half an equivalent of Na[Au^{III}-Cl₄]·2H₂O in ethanol affords the light-green anion [Au^{III}-(L^{*t*-Bu})₂]⁻. Microcrystalline light-green [N(*n*-Bu)₄][Au-(L^{*t*-Bu})₂] (**1**) has been isolated in 72% yield after addition of [N(*n*-Bu)₄]Br. Complex **1** is as expected diamagnetic ($S = 0$) since it contains a Au^{III} ion (d⁸) in a square planar S₄ ligand field.

Figure 1 displays the electronic spectrum of **1** in CH₂Cl₂ which exhibits two d–d transitions in the visible at 415–(227) and 618 nm ($\epsilon = 80$ M⁻¹ cm⁻¹) of low intensity. This is in perfect agreement with other known diamagnetic square planar complexes of Au^{III} with a d⁸ electron configuration.¹⁴

By using the unsubstituted ligand 1,2-benzenedithiolate in this reaction and adding tri(*n*-butyl)amine, the salt [NH-(*n*-Bu)₃][Au^{III}(L)₂] (**2**) has been prepared, and single crystals suitable for X-ray crystallography have been obtained. The structure of the oxidized product, namely [Au(L)₂], has been reported in ref 10.

We have determined the crystal structure of **2** at 100(2) K by using Mo K α radiation. Figure 2 shows schematically the important structural features, and Table 2 summarizes bond lengths. The [NH(*n*-Bu)₃]⁺ cation and two crystallographically distinct [Au^{III}(L)₂]⁻ anions (each located on a special position) are present in **2**. One of these anions is not involved in hydrogen bonding contacts to the cation; only a very weak sulfur···sulfur contact at 3.475(3) Å between the two anions exists. The other anion forms two weak N–H···S bonds at 3.322(3) Å. Figure 3 shows the structure of the square planar anion which is not involved in hydrogen bonding and gives the bond distances. It is important to note

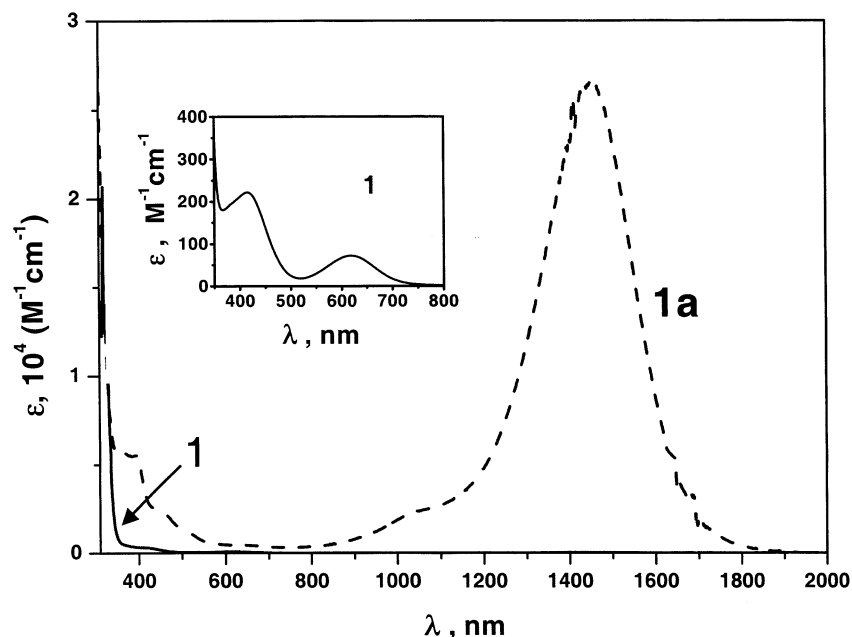


Figure 1. Electronic spectra of **1** in CH_2Cl_2 and chemically generated **1a** in CH_2Cl_2 solution (0.10 M $[\text{N}(n\text{-Bu})_4]\text{PF}_6$). The insert shows the spectrum of **1** in the visible region.

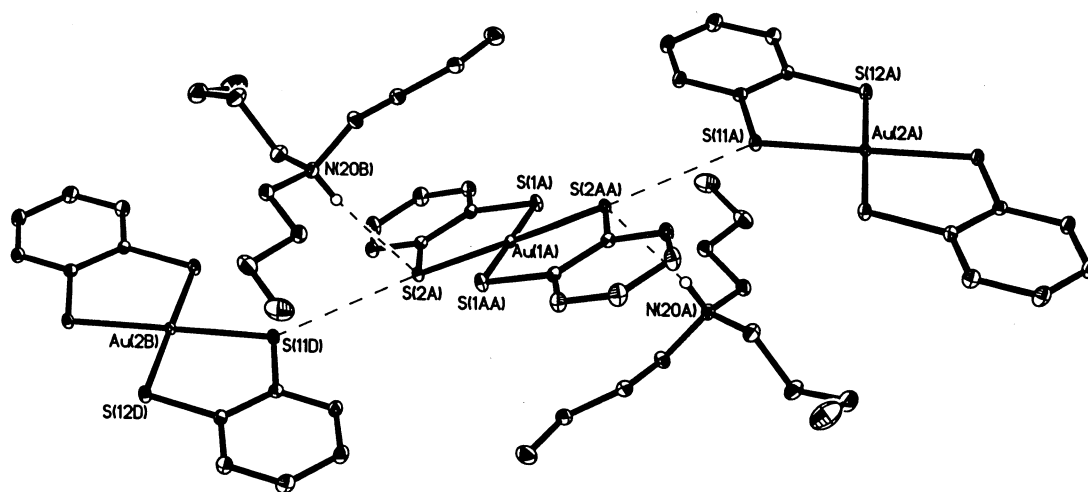


Figure 2. Structure of the two distinct $[\text{Au}(\text{L})_2]^-$ anions and their $[\text{N}(n\text{-Bu})_3\text{H}]^+$ cations in crystals of **2**. The $\text{N}\cdots\text{S}$ hydrogen contacts at 3.322(3) Å and the $\text{S}\cdots\text{S}$ contact at 3.475(3) Å are shown as dotted lines.

Table 2. Selected Bond Distances (Å) in **2**

Au1–S1	2.3162(5)	Au2–S11	2.3051(6)
Au1–S2	2.3027(5)	Au2–S12	2.3139(5)
S1–C1	1.760(2)	S11–C11	1.764(2)
S2–C2	1.768(2)	S12–C12	1.764(2)
C1–C6	1.398(3)	C11–C16	1.402(3)
C1–C2	1.403(3)	C11–C12	1.397(3)
C2–C3	1.403(3)	C12–C13	1.397(3)
C3–C4	1.383(3)	C13–C14	1.386(3)
C4–C5	1.397(3)	C14–C15	1.392(3)
C5–C6	1.386(3)	C15–C16	1.382(3)

that both C–S bonds in an $(\text{L})^{2-}$ ligand are equidistant and long at 1.764(2) Å. The six C–C distances of the phenyl ring are also equidistant within experimental error. The average C–C distance at 1.393(3) Å is typical for an aromatic phenyl ring. Interestingly, in $[\text{Ni}(\text{L}^{\text{t-Bu}})_2]^{2-}$, the corresponding metrical parameters of the coordinated $(\text{L}^{\text{t-Bu}})^{2-}$ ligand are very similar indeed^{4b} (see Scheme 2). In particular,

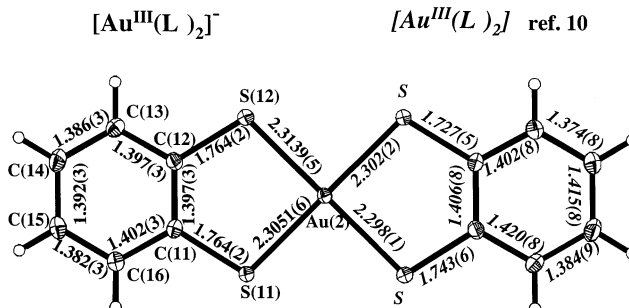


Figure 3. Schematic representation of the anion without hydrogen bonding contacts in crystals of **2** (non-hydrogen atoms are drawn at the 70% probability level). The bond distances on the left-hand side of the molecule are those of **2** whereas those given in italics on the right-hand side are those of the neutral molecule $[\text{Au}(\text{L})_2]$ reported for **2a** from ref. 10.

the C–S bonds at average length 1.762 Å are long and indicate the presence of S,S-coordinated aromatic 1,2-dithiolate ligands.

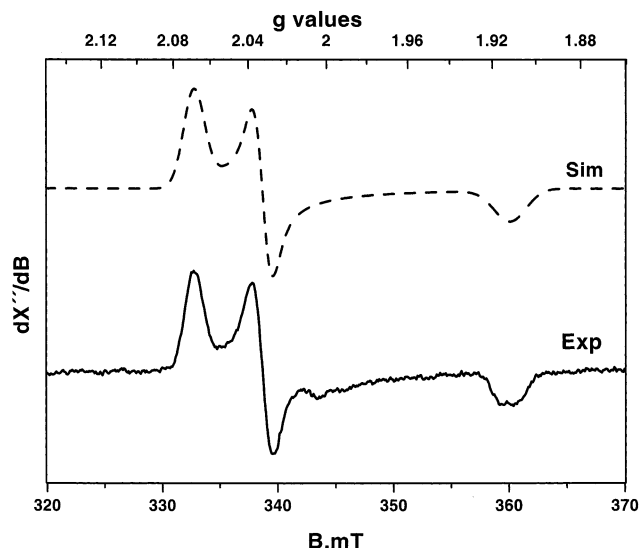


Figure 4. X-band EPR spectrum of chemically generated **1a** in frozen CH_2Cl_2 solution at 30.1 K. Conditions: frequency 9.6355 GHz; modulation 10.0 G, power $504 \mu\text{W}$. For simulation parameters ($W_x = 25.0$, $W_y = 19$, $W_z = 35$ Hz), see text.

It is therefore significant that the geometrical parameters of the S,S-coordinated ligands in $[\text{Au}(\text{L})_2]^{10}$ are different from those in **2**. As shown in Figure 3, the neutral molecule is also planar, but the average C–S bond at $1.735(6) \text{ \AA}$ is significantly shorter and the C–C bonds show an alternating pattern of two shorter C=C bonds (av 1.380 \AA) and four longer ones at av 1.406 .¹⁰ Interestingly, the av Au–S bond in **2** at 2.309 \AA is nearly the same as in $[\text{Au}(\text{L})_2]$ (**2a**) at 2.300 \AA . The observed distortions of the $(\text{L})^{2-}$ ligands in $[\text{Au}(\text{L})_2]$ are the arithmetic average of those in $[\text{Ni}(\text{L}^t\text{-Bu})_2]$ and $[\text{Ni}(\text{L}^t\text{-Bu})_2]^{2-}$ (Scheme 2) and are as observed in $[\text{Ni}^{\text{II}}(\text{L}^t\text{-Bu})(\text{L}^t\text{-Bu})]^-$.^{4b} These observations represent clear evidence that the neutral molecule $[\text{Au}(\text{L})_2]$ consists of a diamagnetic Au^{III} ion (d^8) and one 1,2-dithiobenzosemiquinonate radical anion and one 1,2-dithiolate($2-$) ligand. Note that crystallographically the two ligands are identical which implies a delocalized mixed valent electronic structure (class III).

Complex **1** was chemically oxidized with iodine in acetone. The obtained yellow-green, microcrystalline $[\text{Au}(\text{L}^t\text{-Bu})_2]$ (**1a**) is paramagnetic, whereas solid **2a** is diamagnetic.¹⁰ Temperature-dependent (4–300 K) magnetic susceptibility measurements using a SQUID magnetometer in an external magnetic field of 1.0 T indicated a temperature-independent (10–300 K) magnetic moment of $1.73 \mu_{\text{B}}$ ($S = 1/2$) and $g = 2.0$ for **1a**. This result immediately implies that the paramagnetic neutral molecules in **1a** do not pack in the solid state in a fashion giving rise to intermolecular spin exchange phenomena. In particular, no dimer formation as in $[\text{Au}(\text{L})_2]$ is possible.

The $S = 1/2$ ground state for **1a** is confirmed by the X-band EPR spectrum of a frozen CH_2Cl_2 solution at 30.1 K shown in Figure 4. This shows that **1a** does not dimerize, even in solution. A rhombic signal with $g_x = 2.0690$, $g_y = 2.0320$, $g_z = 1.911$ ($g_{\text{iso}} = 2.0030$) has been observed without detectable ^{197}Au ($I = 3/2$, 100% natural abundance) hyperfine splitting. This rules out the presence of a Au^{IV} ion with low

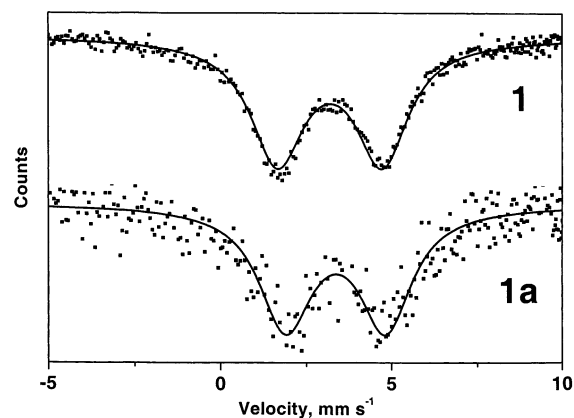


Figure 5. ^{197}Au Mössbauer spectra of **1** and **1a** at 4.2 K.

spin d^7 electron configuration ($S_{\text{Au}} = 1/2$). Note that the EPR spectra of some mononuclear Au^{II} (d^9 , $S_{\text{Au}} = 1/2$) complexes have been reported. For instance, the spectrum of $[\text{Au}^{\text{II}}(\text{9-aneS}_3)_2](\text{BF}_4)_2$ has been reported.¹⁵ $g_1 = 1.9888$, $g_2 = 2.0042$, $g_3 = 2.0407$ ($g_{\text{iso}} = 2.0106$) and $A_1(^{197}\text{Au}) = -35 \times 10^{-4}$, $A_2 = 55 \times 10^{-4}$, $A_3 = -43 \times 10^{-4} \text{ cm}^{-1}$ ($A_{\text{av}}(^{197}\text{Au}) = -41 \times 10^{-4} \text{ cm}^{-1}$). More relevant to the present investigation are the EPR spectra of square planar $[\text{Au}^{\text{II}}(\text{mnt})_2]^{2-}$ where mnt^{2-} represents 1,2-dicyanoethene-1,2-dithiolate($2-$).¹⁶ The X-band EPR spectrum ($g_x = 1.9784$, $g_y = 2.0064$, $g_z = 2.0168$; $A_x(^{197}\text{Au}) = -39.6 \times 10^{-4}$, $A_y(^{197}\text{Au}) = -40.4 \times 10^{-4}$, $A_z(^{197}\text{Au}) = -41.2 \times 10^{-4} \text{ cm}^{-1}$) has been interpreted in terms of a Au^{III} with a radical anion ligand,¹⁷ but see ref 16b where the magnetic orbital has been analyzed to have 20% Au character in agreement with the large ^{197}Au hyperfine coupling. The EPR spectrum of **1a** is only in accord with a formulation as Au^{III} and an S,S-coordinated *o*-dithiobenzosemiquinonate($1-$) radical. This is in excellent agreement with the EPR spectrum reported for $[(\text{bpy})\text{Pd}^{\text{II}}(\text{L}^t\text{-Bu})]^+$ where again no Pd hyperfine coupling has been observed ($g_1 = 2.018$, $g_2 = 2.006$, $g_3 = 1.993$; $g_{\text{iso}} = 2.0057$).⁵

It is well established that ^{197}Au Mössbauer spectroscopy is a useful and sensitive tool for the elucidation of coordination numbers and oxidation states of gold ions in coordination compounds.¹⁸ Therefore, we have recorded the ^{197}Au Mössbauer spectra of **1** and **1a** at 4.2 K (Figure 5) and established the following Mössbauer parameters for **1**, isomer shift $\delta = 3.36 \text{ mm s}^{-1}$, quadrupole splitting $\Delta E_{\text{Q}} = 2.92 \text{ mm s}^{-1}$, and for **1a**, $\delta = 3.20 \text{ mm s}^{-1}$, $\Delta E_{\text{Q}} = 3.06 \text{ mm s}^{-1}$. Thus, one-electron oxidation of **1** to **1a** does not affect the Mössbauer parameters greatly, and certainly, a change of the d^n electron configuration from d^8 in **1** to d^7 (low spin) in **1a** is clearly not in accord with the data. In fact, the data nicely corroborate a $\text{Au}^{\text{III}}\text{S}_4$ structure in both cases.¹⁸

Figure 6 displays the infrared spectra (KBr disks) of **1** and **1a** in the range $1500\text{--}500 \text{ cm}^{-1}$. The spectra are as expected quite similar with the notable exception that **1a**

(15) Ihlo, L.; Kampf, M.; Böttcher, R.; Kirmse, R. *Z. Naturforsch.* **2002**, *57b*, 171.

(16) (a) Van Reus, J. G. M.; Vieggers, M. P. A.; de Boer, E. *Chem. Phys. Lett.* **1974**, *28*, 104. (b) Ihlo, L.; Stösser, R.; Hofbauer, W.; Böttcher, R.; Kirmse, R. *Z. Naturforsch.* **1999**, *54b*, 597.

(17) Schlupp, R. L.; Maki, A. H. *Inorg. Chem.* **1974**, *13*, 44.

(18) Parish, R. V. *Gold Bull.* **1982**, *15*, 51.

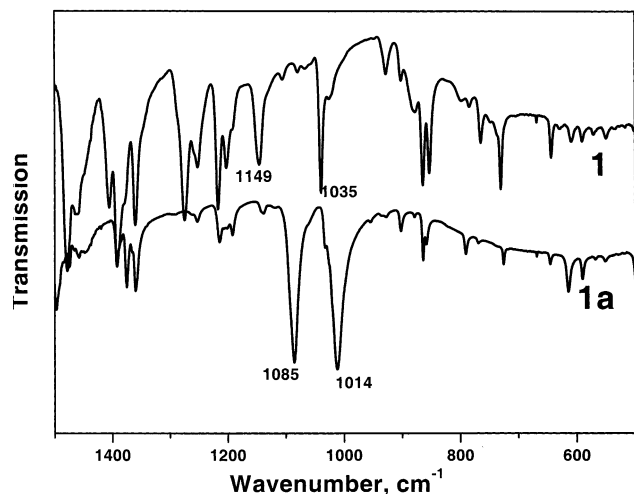


Figure 6. Infrared spectra of **1** and **1a** (KBr disks) in the region 500–1500 cm^{-1} .

exhibits two strong new bands at 1085 and 1014 cm^{-1} , both of which are absent in the spectrum of **1**. We assign these bands to predominantly $\nu(\text{C}=\text{S}^{\bullet})$ stretching frequencies of S,S'-coordinated *o*-dithiobenzosemiquinonate(1 $^{-}$) radicals. This is in accord with a resonance Raman investigation of the phenylthiyl radical¹⁹ for which the predominantly $\nu(\text{C}=\text{S}^{\bullet})$ mode has been observed at 1073 cm^{-1} (ν_{7a} Wilson mode). These intense bands in the region 1100–1000 cm^{-1} are spectroscopic markers for the occurrence of *o*-dithiobenzosemiquinonate radicals. Thus, in $[\text{N}(n\text{-Bu})_4][\text{Co}^{III}(\text{L}^t\text{-Bu})_2]$,²⁰ these bands are *not* observed since it contains two *o*-dithiophenolate(2 $^{-}$) ligands and a cobalt(III) ion, but in Sellmann's complex $[\text{N}(n\text{-Bu})_4][\text{Ni}^{II}(\text{L}^t\text{-Bu})(\text{L}^t\text{-Bu}^{\bullet})]$, an intense band at 1114 cm^{-1} is observed.^{4b,20} The fact that **1a** displays two such bands may point to the existence of two isomers of $[\text{Au}^{III}(\text{L}^t\text{-Bu})(\text{L}^t\text{-Bu}^{\bullet})]$, namely a *trans*- and a *cis*-isomer. Lacking a crystal structure of **1a**, we cannot prove this point at present.

Figure 7 displays the cyclic voltammogram of **1** in CH_2Cl_2 solution containing 0.10 M $[\text{N}(n\text{-Bu})_4]\text{PF}_6$ supporting electrolyte. The redox potentials are referenced versus the ferrocenium/ferrocene (Fc^+/Fc) couple. Two reversible one-electron transfer processes are observed at 0.074 and -2.28 V versus Fc^+/Fc . Coulometric measurements established that the first process corresponds to a (ligand-centered) one-electron oxidation of **1** whereas the second is most likely a metal-centered one-electron reduction, eq 1.

Since the one-electron oxidized form of **1** is stable in CH_2Cl_2 solution, we have been able to record the electronic spectrum of **1a** which is shown in Figure 1. It is interesting that this species displays a very intense absorption maximum

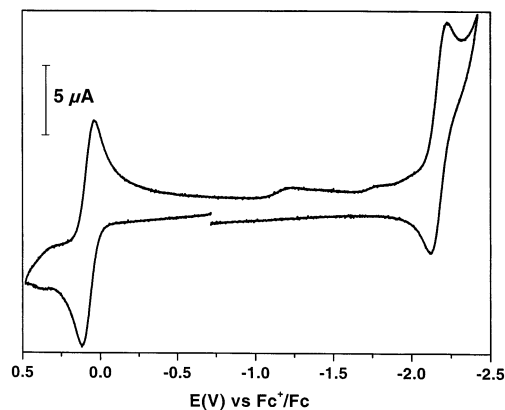
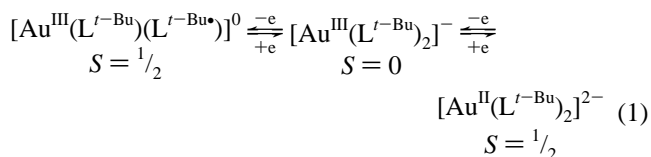


Figure 7. Cyclic voltammogram of **1** in CH_2Cl_2 solution (0.10 M $[\text{N}(n\text{-Bu})_4]\text{PF}_6$) at a glassy carbon working electrode at 200 mV s^{-1} scan rate and 20 $^{\circ}\text{C}$.



in the near-infrared region at 1452 nm ($\epsilon = 2.7 \times 10^4 \text{ M}^{-1} \text{ s}^{-1}$) and, in addition, maxima at 400 nm ($5.6 \times 10^3 \text{ M}^{-1} \text{ cm}^{-1}$) and 1023 nm ($2.2 \times 10^3 \text{ M}^{-1} \text{ cm}^{-1}$). We tentatively assign the intense band at 1452 nm to an intervalence transition of the type $[\text{Au}^{III}(\text{L}^t\text{-Bu})(\text{L}^t\text{-Bu}^{\bullet})] \rightleftharpoons [\text{Au}^{II}(\text{L}^t\text{-Bu})(\text{L}^t\text{-Bu}^{\bullet})]$. Note that $[\text{AsPh}_4][\text{Ni}^{II}(\text{L}^t\text{-Bu})(\text{L}^t\text{-Bu}^{\bullet})]$ displays this intervalence transition at 860 nm ($\epsilon = 1.2 \times 10^4 \text{ M}^{-1} \text{ cm}^{-1}$);^{4b} it is absent (>700 nm) in $[\text{N}(n\text{-Bu})_4][\text{Co}^{III}(\text{L}^t\text{-Bu})_2]$.²⁰

In summary, we have established that the electronic structure of complexes **1a** and **2a** cannot be described as species containing a central Au(IV) ion with a low spin d^7 electron configuration. Rather, these square planar paramagnetic ($S = 1/2$) species contain an S,S'-coordinated 1,2-dithiobenzosemiquinonate(1 $^{-}$) radical. Spectroscopic and structural markers for such radicals are the following: (i) There are a short C–S bond at $\sim 1.72 \text{ \AA}$ and a quinoid type distortion of the six-membered ring giving rise to two relatively short, alternating C–C bonds and four longer C–C bond distances. (ii) In the infrared, there is a $\nu(\text{C}=\text{S}^{\bullet})$ stretching frequency at $\sim 1100 \text{ cm}^{-1}$. (iii) In the near-infrared, **1a** displays an intense ligand intervalence band at 1452 nm. (iv) The EPR signal of **1a** does not exhibit Au hyperfine coupling nor coupling to the hydrogen atoms of the phenyl ring; it is characteristic of an S-centered radical.

Acknowledgment. We thank the Fonds der Chemischen Industrie for financial support.

Supporting Information Available: Crystal data, final coordinates; temperature factors, distances, and angles for the crystallographic study of **2**. This material is available free of charge via the Internet at <http://pubs.acs.org>.

(19) Tripathi, G. N. R.; Sun, Q.; Armstrong, D. A.; Chipman, D. M.; Schuler, R. H. *J. Phys. Chem.* **1992**, *96*, 5344.

(20) Ray, K.; Wieghardt, K. Unpublished results.